Development of 2.4-GHz film bulk acoustic wave filter for wireless communication

Chi-Ming Fang
National Taiwan University
Institute of Applied Mechanics
1, Sec. 4, Roosevelt Road
Taipei 106, Taiwan

Shih-Yung Pao
National Taiwan University
Institute of Applied Mechanics
1, Sec. 4, Roosevelt Road
Taipei 106, Taiwan
E-mail: sypao@mems.iam.ntu.edu.tw

Chi-Yuan Lee
Yuan Ze University
Department of Mechanical Engineering
Fuel Cell Research Center
135 Yuan-Tung Road, Chungli
320 Taoyuan, Taiwan

Yi-Chang Lu
Asia Pacific Microsystems, Inc.
No. 2, R&D Road 6
Science-Based Industrial Park
Hsinchu, Taiwan

Pei-Yen Chen
Chung-Shan Institute of Science and Technology
Materials and Electro-Optics Research Division
P.O. Box 90008-8-6
Lung-Tan
Tao-Yuan 325, Taiwan

Yung-Chung Chin
TXC Corporation
4 Kung Yeh 6th Road
Cheng City
Tao Yuan 324, Taiwan

Pei-Zen Chang
National Taiwan University
Institute of Applied Mechanics
1, Sec. 4, Roosevelt Road
Taipei 106, Taiwan

Abstract. This research shows the realization of 2.4-GHz film bulk acoustic wave (FBAW) filters. The design, simulation, fabrication, measurement, and analysis of the film bulk acoustic wave resonator (FBAR) devices are covered, which is helpful for the manufacture of the FBAR devices. The simulation of the FBAR and RF circuitry can be integrated on a single platform. The fabrication of the FBAW filters is compatible with complementary metal-oxide semiconductors. This device can be used in 2.4-GHz bandpass filters, such as 802.11b/g and Bluetooth. In this research, the 2.4-GHz FBAW filters for wireless communication have been accomplished. The fabricated FBAW filters have insertion loss of –10 dB, return loss of –7 dB, and stopband rejection of –25 dB, central frequency of 2.485 GHz, bandwidth of 60 MHz, and size of 0.5 mm × 0.5 mm.
[DOI: 10.1117/1.3094749]

Subject terms: film bulk acoustic wave resonator; film bulk acoustic wave filter; radiofrequency filter; complementary metal-oxide semiconductor microelectromechanical systems; radiofrequency microelectromechanical systems.

Paper 08106SSR received Aug. 14, 2008; revised manuscript received Nov. 22, 2008; accepted for publication Dec. 8, 2008; published online Apr. 8, 2009.

1 Introduction

With the development of the wireless communication, a high performance radio frequency (RF) bandpass filter will be needed. Film bulk acoustic wave (FBAW) filter has many advantages, such as small size, low insertion loss, high frequency operation, and complementary metal-oxide semiconductor (CMOS) compatibility. Therefore, it has the potential to be the RF bandpass filter in the next generation of devices.

In the 1980s, the first film bulk acoustic resonator (FBAR) was presented, and the working frequency was about 200 MHz.[1] In the 1990s, the gigahertz FBAR was presented.[2] In this paper, the FBARs connecting some inductors and capacitors are used for the gigahertz filter application. Also in the 1990s, FBARs were integrated with a

1932-5150/2009/$25.00 © 2009 SPIE

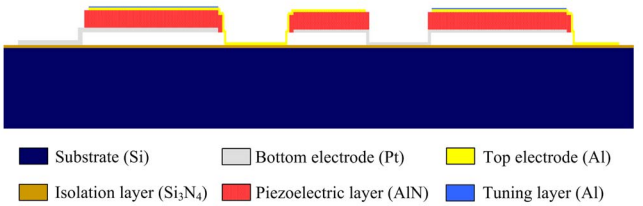

Fig. 1 The schematic of FBAW filters structure.

heterojunction-bipolar-transistor amplifier on a GaAs substrate.[3] The modified Butterworth-Van Dyke model for parameter extraction of FBARs was presented,[4] and it is helpful for characteristics analysis of FBAR. In this phase, these researchers were focused on characteristics analysis of FBARs and chasing its valuable applications. In the 2000s, with the vast development of wireless communication field, the study of FBAR devices for a communications application became more and more emphasized. The FBAR duplexer for United States Personal Communications Service handset was presented in 2001.[5] The FBAW filters for 5-GHz were presented in 2002,[6] and their size is one-tenth of traditional ceramic filters. In 2003, FBARs applied to high frequency oscillators were presented.[7] The development trend of the FBAW filter in the monolithic RF front-end in a communications system were presented in 2004.[8] Then FBAW filters for a wideband code division multiple access mobile phone and FBAW filters integrated with RF front-end circuits were presented.[9,10] This showed that the FBAW filters were integrated with RF circuits by above integrated circuit (IC) technique, thus the fully integrated RF front-end was feasible. A FBAW filter applied to RF receiver front-end was presented in 2006,[11] which showed that the design of a 2.4-GHz FBAW filter, and the filter, could be used in 802.11b/g systems and blutooth systems. Design and simulation of FBAW filters at high frequency bands (*X* band) were presented in 2007.[12] This showed that high frequency FBAW filters were simulated in Advanced Design System ([ADS] Agilent technologies, Santa Clara, California) momentum software.

In this study, the 2.4-GHz FBAW filters have been achieved. The cross-sectional view of FBAW filter structure is shown in Fig. 1. It can be used in 2.4-GHz bandpass filters, such as 802.11b/g and Bluetooth. In addition, this paper constructs a complete process from design to fabrication of FBAW filters. This paper demonstrates that FBAR devices have the capability to integrate with RF circuitry.

2 Design and Simulation

During our research phase, we determined the FBAW filters should conform to 2.4-GHz wireless communication protocol. For this purpose, the desired impedance is 50 Ω, and the central frequency is 2450 MHz in the filter design. The bandwidth is about 80 MHz. Attenuation in stopband is at least −30 dB; insertion loss is within −3 dB.

2.1 *Modeling of Resonator*

A FBAW filter consists of several FBARs. The basic structure of a FBAR includes a bottom electrode layer, a top electrode layer, and a piezoelectric layer sandwiched between them as shown in Fig. 2.

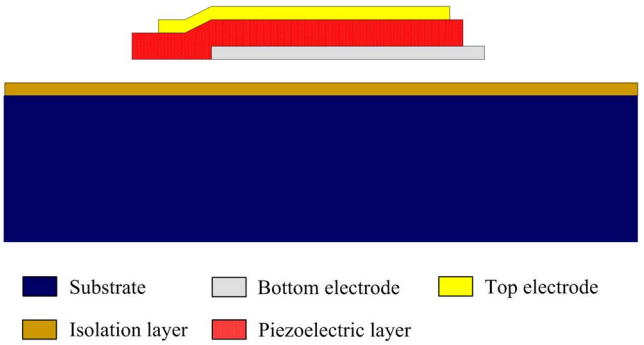

Fig. 2 The schematic of basic multilayer FBARs structure.

Many methods were presented in the past to solve the problem of acoustic waves propagating in FBARs with multilayers. Among them, an exact equivalent circuit model was presented by Mason in 1948[13] and is shown in Fig. 3. However, the inclusion of transformer and a negative capacitance in the Mason model imposes difficulties in circuit simulation software. Besides, the acoustic and electric losses of piezoelectric thin film, metal layers, and a structure layer are not considered in the Mason equivalent circuit model. To model the layered FBAR structure exactly, this paper adopts the concept of the Mason model and KLM (or Krimholtz-Leedom-Mattheci) model to build on FBAR equivalent circuit model.[14]

By use of a network analytical method, the characteristics of FBAR can be simulated by a numerical analysis program such as MATLAB software (The Mathworks, Natick, Massachusetts). In order to consider losses and the parasitic effect in the simulation, the Mason equivalent circuit model will be modified. First, the imaginary part is added in the mechanical impedance of each layer and wave number. It is modified by the acoustic loss term, which is related with quality factor Q and an attenuation factor. Next, the capacitance of resonator is modified by an imaginary part, which is from the dielectric loss term ρ of piezoelectric film. Finally, the series resistance from the electrode layer is separated on both sides of the resonator port. The characteristics of FBAR can be simulated more exactly by the modified Mason equivalent circuit model.

The simulation results have been verified with the experimental results. Furthermore, to make it feasible to use the FBAR model in circuit design, the FBAR resonator

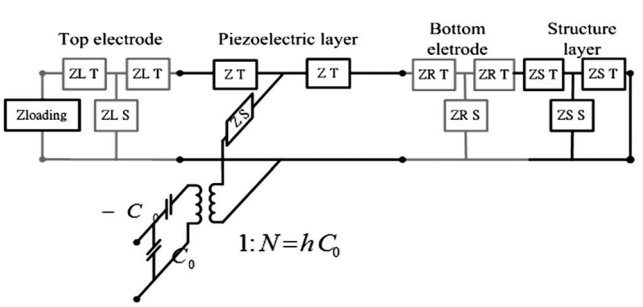

Fig. 3 The Mason equivalent circuit model of FBARs.

model is built up as a functional block in the ADS software. Then, FBAR can be taken as a circuit component and used in RF IC design.

2.2 *Filter Design Procedure*

A ladder-type filter is used to meet the desired specification. It is composed of the serial and parallel FBAR resonators. There are two design methods adapted to design RF filters by use of lumped-element circuits conventionally.

One is the image parameter method. First, the simplest 1×1 filter is designed by choosing the image impedances of both ends of the 50-Ω transmission line at the central frequency of the filter. It can be shown that the image impedances of both ends are the same for the symmetry of the FBAR filter. The product of the areas of the serial and parallel FBAR resonators can be determined. Next, the stopband rejection of the filter can be increased by cascading the simplest 1×1 filter imaginarily. Finally, by using a numerical simulation procedure, the ratio of the areas of the serial and parallel FBAW resonators can be determined by the bandwidth of the filter. The advantages of this method are (i) an easier design than is used with the insertion loss method and (ii) it has the same area size of the resonator pairs. However, it needs more pairs to achieve the standard of stopband rejection and fewer ripples in the passband.

In this paper, the insertion loss method is adopted to design the filter structure. In this method, it is assumed that one-dimensional model is adequate to express FBAR characteristics. The impedance of FBAR behaves like a capacitance with infinite pole and zero pairs. If the effect of force loaded on both electrodes of the FBAR impedance model is ignored, the FBAR impedance can be simplified as

$$Z=\frac{1}{j\omega C}\left(1-k_t^2\frac{\tan\dfrac{d\omega}{2V}}{\dfrac{d\omega}{2V}}\right), \tag{1}$$

where

$$k_t^2=\frac{h_{Z3}^2\varepsilon_{zz}^S}{C_{33}^D},\quad V=\sqrt{\frac{C_{33}^D}{\rho}},\quad C=\frac{A\varepsilon_{zz}^S}{d}. \tag{2}$$

The coefficient k_t^2 is electromechanical coupling coefficient, h_{Z3}^2 is piezoelectric coupling coefficient, C_{33}^D is elastic constant, ε_{zz}^S is dielectric constant, ρ is density, V is velocity, d is thickness, and A is area.

Then, for a series-connected inductor-capacitor (LC) tank, if the impedance of FBAR could be taken as an LC resonator, the characteristic of impedance must to be as follows:

$$Z(\omega_0)=Z_S(\omega_0)=0$$

$$\frac{d}{d\omega}Z(\omega_0)=\frac{d}{d\omega}Z_S(\omega_0)=j2L=j\frac{2}{\omega_0^2C}. \tag{3}$$

If we substitute Eq. (3) into Eq. (1), the thickness and area size of FBAR can be determined. However, the thickness calculated from a simplified equation is not very exact. The thickness of each layer should be chosen by the modified Mason model. The thickness and area size of FBAR can be determined by

$$d=2x\frac{V}{\omega_0}$$

$$A=\frac{\dfrac{x^2}{k_t^2}+k_t^2-1}{\omega_0\varepsilon_{zz}^S}xVC\quad x\cot x=k_t^2. \tag{4}$$

Similarly, for a shunt-connected LC tank, the characteristic of impedance must to be as follows:

$$Y(\omega_0)=Y_P(\omega_0)=0$$

$$\frac{d}{d\omega}Y(\omega_0)=\frac{d}{d\omega}Y_P(\omega_0)=j2C=\frac{j2}{\omega_0^2L}. \tag{5}$$

If we substitute Eq. (5) into Eq. (1), the thickness and area size of FBAR can be determined as follows:

$$d=\pi\frac{V}{\omega_0}$$

$$A=\frac{8k_t^2}{\pi}\frac{VC}{\omega_0\varepsilon_{zz}^S}. \tag{6}$$

The size can be preliminarily determined using Eqs. (4) and (6).

In general, the Butterworth and Chebyshev types are usually used for filter designs. The value of inductance and capacitance of ideal series and parallel LC tank can be calculated by basic filter theory.[15] Then, each FBAR area of the filter can be determined by fitting the impedance of the LC tank.

Butterworth function method is used to design the FBAW filter in this case. Following the Previously described procedures, each parameter of the FBAR components constituting the desired filter is obtained as listed in Table 1.

2.3 *Simulation*

In general, the Butterworth and Chebyshev types are usually used to filter designs, and Butterworth type is used in this case. The simulation model is built up as a functional block in the ADS software. Therefore, the FBAR device can be simulated accurately and taken as a lump component to be used in RF IC design. The simulation results of designed third-order (two-by-one) and fifth-order (three-by-two) ladder-type filters are shown in Fig. 4. Figure 4 shows that the passband is about 2410 to 2480 MHz; insertion loss is within −3 dB; return loss is smaller than −15 dB, attenuation in stopband is smaller than −18 dB. The stopband rejection of fifth-order filter is better than that of third-order, but the size of fifth-order is larger than that of third-order. The simulation results of various filters are listed in Table 1.

Table 1 The parameters of each FBAR in designed filter.

Parameter	Third-order filter		Fifth-order filter		
Filter type	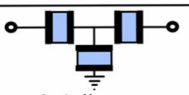 2×1 discrete		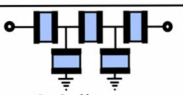 3×2 discrete		
FBAR unit	serial	shunt	serial	shunt	serial
Area size (μm^2)	103^2	229^2	123^2	218^2	68^2
Bottom electrode (Ti/Pt) (nm)	10/100	10/100	10/100	10/100	10/100
Piezoelectric layer (AlN) (nm)	1400	1400	1400	1400	1400
Top electrode (Al) (nm)	150	210	150	210	150
Passband	2410 to 2480 MHz		2408 to 2478 MHz		
Attenuation in stopband	-18 dB		-35 dB		
Attenuation rate near the bandwidth	1.6 dB @ 1 MHz		2.0 dB @ 1 MHz		

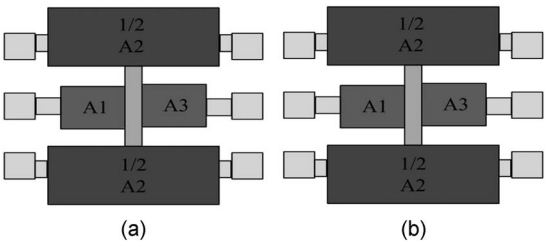

Fig. 5 Layout schematics of FBAW filters. (a) Third-order ladder type. (b) Fifth-order ladder type.

3 Fabrication Method

3.1 *Structure Layout and Process Consideration*

The layouts of desired third-order and fifth-order ladder-type FBAW filters are shown in Fig. 5. As shown in this layout, the symmetry of the structure can help reduce high frequency parasitic effect. Therefore, parts of resonators are divided into two symmetric lumps. The emphasis of FBAW filter fabrication would be the compatibility of micro-electro-mechanical systems process and CMOS standard IC process. Therefore, the material and etching selectivity of each layer are considered. In the experiment, the well-oriented quality of piezoelectric layer sputtering is critical, and side etching of the piezoelectric layer needs to be reduced. Certainly, the circuit protection and temperature limitation are regarded during the post-IC process.

3.2 *CMOS Compatible Micro-Electro-Mechanical Systems Process*

This fabrication is used for the surface micromachining process. The FBAW filters are air-gap suspended, and the detail fabrication flow is shown in Fig. 6.

First, the isolation layer (Si_3N_4) is developed, and the sacrificial layer (Al) is deposited and patterned. Second, the thin film of bottom electrode (Pt) is deposited on the sacrificial layer, and it is patterned by lift-off method. A uniform bottom would be helpful for excellent piezoelectric deposition. Then, a well-oriented piezoelectric layer (AlN) is sputtered on the patterned bottom electrode. The tempera-

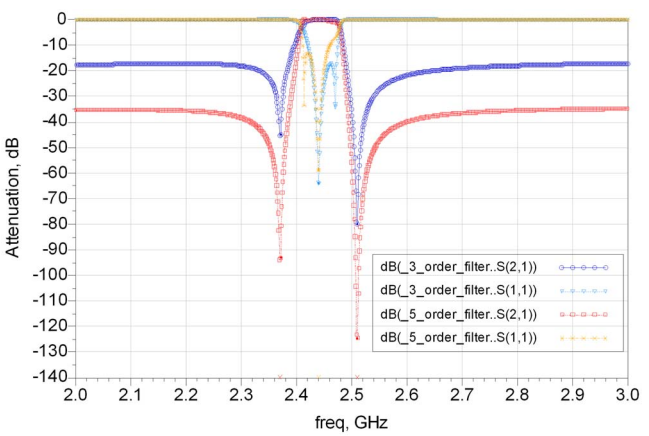

Fig. 4 Simulation results of 2.4-GHz FBAW filters. It contains S_{21} and S_{11} of third-order and fifth-order filters.

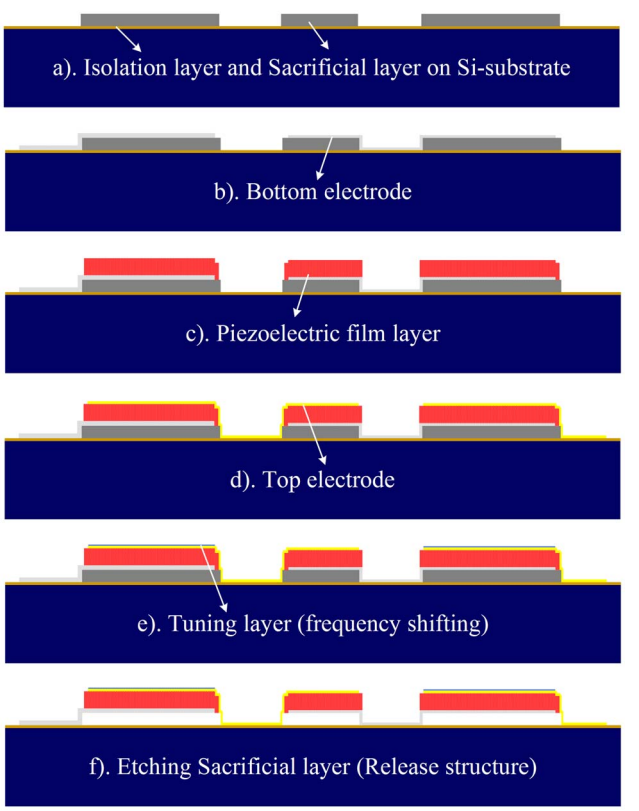

Fig. 6 The CMOS-compatible FBAW filters fabrication process.

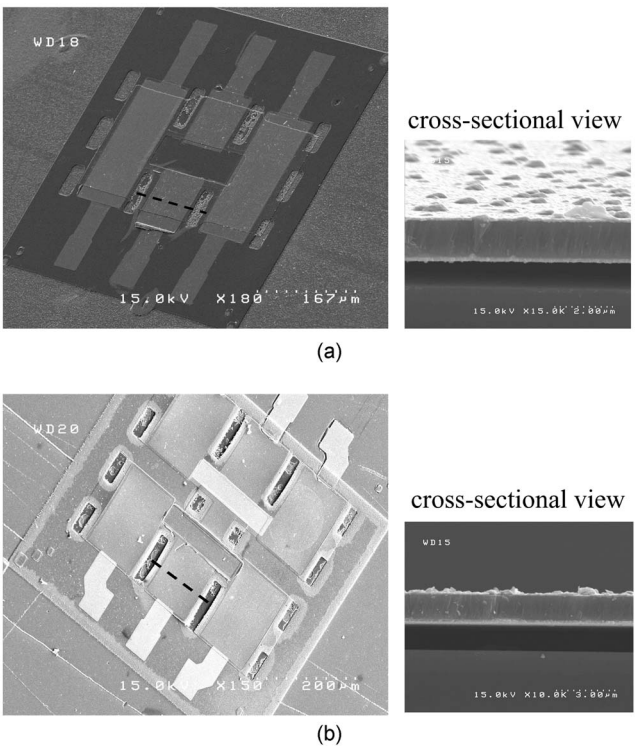

Fig. 7 Scanning electron microscopy images of the accomplished FBAW filters. (a) The third-order FBAW filter and its enlarged cross-sectional view along section line. (b) The fifth-order FBAW filter and its enlarged cross-sectional view along section line.

ture is limited to approximately 300°C. Finally, the top electrode layer (Al) and the tuning layer (Al) are deposited successively on the piezoelectric layer. After depositing each layer of the FBAW filter, the structure can be released by Al etchant ($H_3PO_4:HNO_3:CH_3COOH:H_2O = 50:2:10:9$).

4 Results and Discussions

The 2.4-GHz FBAW filter has been accomplished, as shown in Fig. 7. Figure 7 shows the structures and cross-sectional view of accomplished third-order and fifth-order FBAW filters. In which, we can confirm that the structure is successfully suspended. The scanning electron microscope and X-ray diffraction diagrams of accomplished FBAW filters are shown in Fig. 8. Figure 8 shows that the piezoelectric layer AlN has good *c*-axial crystal direction in Fig. 8(a). The peak value at the 36-deg phase angle is approximately 11 000 compared with the silicon count 2 200, as shown in Fig. 8(b); therefore, the deposited piezoelectric film AlN has relatively good crystalline quality.

The measured FBAW filter is a third-order filter, and its size is approximately 0.5 mm × 0.5 mm. The measurement results of accomplished FBAW filters are shown in Fig. 9. Figure 9 shows that S_{11} and S_{21} performance of accomplished third-order FBAW filter. Return loss in the passband is smaller than −7 dB. Insertion loss in the passband is approximately −10 dB, and it is worse than expectation. Attenuation in the stopband is approximately −25 dB. The central frequency is 2.485 GHz, and the bandwidth is approximately 60 MHz. The practical stopband rejection (i.e., the difference between attenuation in stopband and insertion loss in passband) is smaller than −15 dB. The measurement and simulation results of FBAW filters are listed in Table 2.

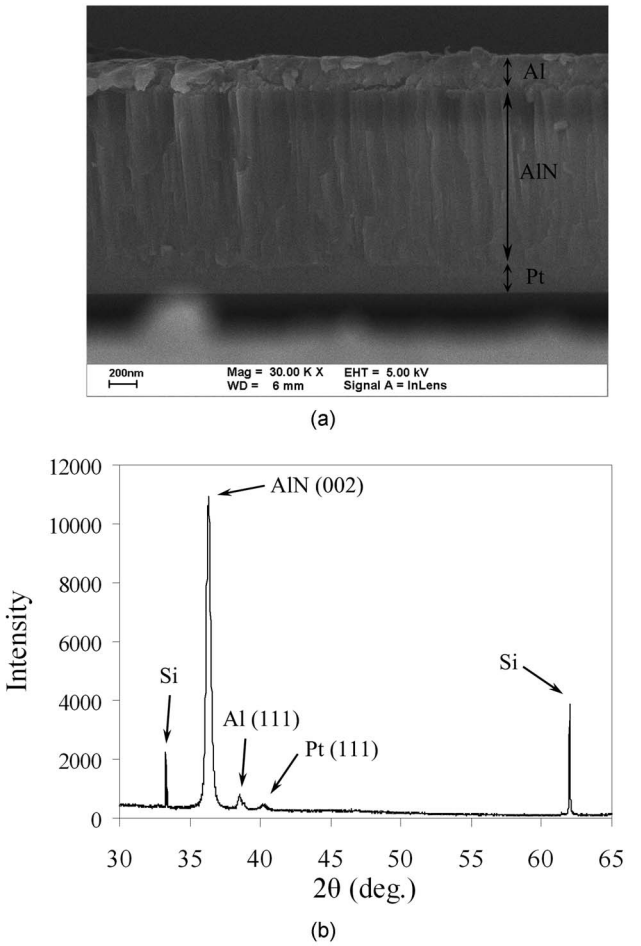

Fig. 8 The quality of piezoelectric film layer AlN. (a) Cross-sectional view of structure. (b) X-ray diffraction diagram of structure.

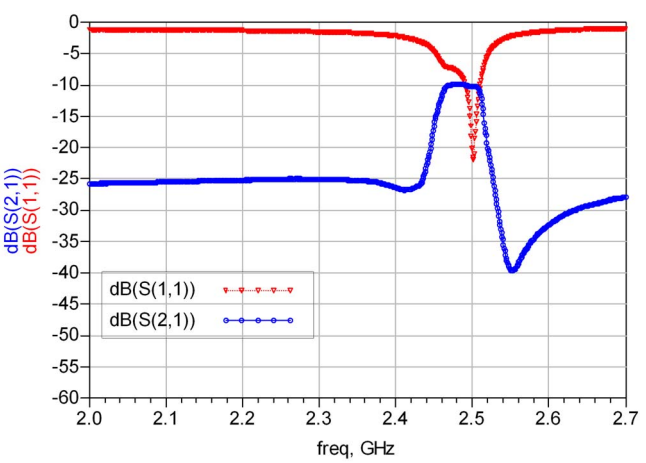

Fig. 9 Measured S_{21} and S_{11} of accomplished third-order FBAW filters.

Table 2 Performance list of measured and designed FBAW filters.

Parameters	Design	Measurement
Central frequency	2.45 GHz	2.485 GHz
Bandwidth	70 MHz	60 MHz
Return loss	<−15 dB	<−7 dB
Insertion loss	within −3 dB	−10 dB
Attenuation in stopband	<−18 dB	<−25 dB

If the accomplished filters did not conform to the requirement, the matching lump element circuits could be applied to the input and output of the filter, and it could be helpful for impedance matching. When we apply various matching circuits to terminals of the accomplished device, the measurement results are shown in Fig. 10. Figure 10 shows the return loss is smaller than −15 dB, and insertion loss is approximately −8 dB. Return loss is improved, and insertion loss is less improved.

5 Conclusions

The 2.4-GHz FBAW filters have been achieved. The fabricated FBAW filters have insertion loss of −10 dB, return loss of −7 dB, and stopband rejection of −25 dB, central frequency of 2.485 GHz, bandwidth of 60 MHz, and size of 0.5 mm × 0.5 mm. In this paper, a complete process from design to fabrication of FBAW filters is constructed. The FBAW filter can be more easily designed, simulated, and fabricated by using the aforementioned method. The FBAR model as a functional block in the ADS software has been built up. It is provided to design and simulate the FBAR device with RF circuitry on a single platform. In addition, fabricating FBAR devices integrated with RF circuitry is feasible. It is promising that FBARs are fully integrated with the RF front-end system on a chip.

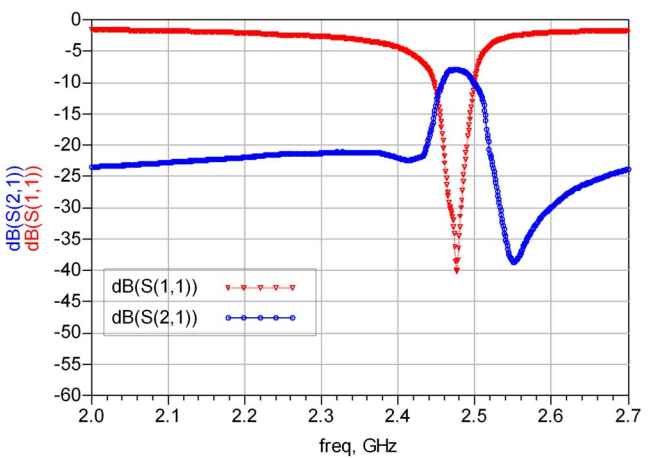

Fig. 10 Measured S_{21} and S_{11} of accomplished third-order FBAW filters with matching circuits. The accomplished FBAW filter connecting with the components of a serial 3nH inductor and a serial 4pF capacitor in input/output terminals, simultaneously.

Acknowledgments

The authors wish to thank Prof. W. P. Shih of the Department of Mechanical Engineering, National Taiwan University, for suggesting the process. We wish to thank P. H. Sung of Electronics Research and Service Organization, Industrial Technology Research Institute of Taiwan, for research guidance. In addition, we wish to thank Y. J. Chen, W. C. Chuang, and H. Z. Lin of Institute of Applied Mechanics, National Taiwan University, for research help. The research was supported by National Science Council of Taiwan.

References

1. K. M. Lakin and J. S. Wang, "Acoustic bulk wave composite resonators," *Appl. Phys. Lett.* **38**(3), 125–127 (1981).
2. C. Vale, J. Rosenbaum, S. Horwitz, S. Krishnaswamy, and R. Moore, "FBAR Filters at GHZ Frequencies," *IEEE Freq. Control Symp.* 332–336 (1990).
3. D. Cushman, K. F. Lau, E. M. Garber, K. A. Mai, A. K. Oki, and K. W. Kobayashi, "SBAR filter monolithically integrated with HBT amplifier," *Proc.-IEEE Ultrason. Symp.* **1**, 519–524 (1990).
4. J. D. Larson III, P. D. Bradley, S. Wartenberg, and R. C. Ruby, "Modified Butterworth-Van Dyke circuit for FBAR resonators, and automated measurement system," *Proc.-IEEE Ultrason. Symp.* **1**, 863–868 (2000).
5. R. C. Ruby, P. Bradley, Y. Oshmyansk, J. D. Chien, and A. Larson, "Thin film bulk wave acoustic resonators (FBAR) for wireless applications," *Proc.-IEEE Ultrason. Symp.* **1**, 813–821 (2001).
6. T. Nishihara, T. Yokoyama, T. Miyashita, and Y. Satoh, "High Performance, and Miniature Thin Film Bulk Acoustic Wave Filters for 5 GHz," *Proc.-IEEE Ultrason. Symp.* **1**, 969–972 (2002).
7. B. P. Otis and J. M. Rabaey, "A 300 μW 1.9 GHz CMOS oscillator utilizing micromachined resonators," *IEEE J. Solid-State Circuits* **38**(7), 1271–1274 (2003).
8. L. Elbrecht, R. Aigner, C. I. Lin, and H. J. Timme, "Integration of bulk acoustic wave filters: concepts, and trends," *IEEE MTTS. Int. Micro. Symp.* Vol. 1, pp.395–398 (2004).
9. M. A. Dubois, C. Billard, C. Muller, G. Parat, and P. Vincent, "Integration of high-Q BAW resonators, and filters above IC," *IEEE Interstate Solid State Circuits Conference (ISSCC)* **1**, 392–606 (2005).
10. J. F. Carpentier et al., "A SiGe:C BiCMOS WCDMA zero-IF RF front-end using an above-IC BAW filter," *IEEE Interstate Soild State Circuits Conference (ISSCC)* **1**, 394–395 (2005).
11. M. El Hassan, C. P. Moreira, A. A. Shirakawa, E. Kerherve, Y. Deval, D. Belot, and A. Cathelin, "A multistandard RF receiver front-end using a reconfigurable FBAR filter," *IEEE Circuits Syst.* 173–176 (2006).
12. A. A. Shirakawa, J. M. Pham, P. Jarry, and E. Kerhervé, "Design of FBAR filters at high frequency bands," *Int. J. RF Microwave Comput.-Aided Eng.* **17**(1), 115–122 (2006).
13. W. P. Mason, *Electromechanical Transducers, and Wave Filters*, Van Nostrand-Reinhold, Princeton, N.J. (1948).
14. R. Krimholtz, D. A. Leedom, and G. L. Matthaei, "New equivalent circuits for elementary piezoelectric transducers," *Electron. Lett.* **6**(13), 398–399 (1970).
15. D. M. Pozar, *Microwave Engineering*, pp. 443–462, Wiley, New York (1998).

Chi-Ming Fang received his BS in civil engineering from National Central University, Jung-Li, Taiwan, in 2003, and his MS from the Institute of Applied Mechanics of National Taiwan University, Taipei, Taiwan, in 2005. Currently, he is a doctoral candidate at the Institute of Applied Mechanics of National Taiwan University, Taipei, Taiwan. His current research focuses on development of film bulk acoustic wave devices and integration of film bulk acoustic wave devices with RF ICs.

Shih-Yung Pao received his BS in civil engineering from the National Taiwan University, Taipei, Taiwan, in 1996, and his MS from the Institute of Applied Mechanics of National Taiwan University, in 1998. In 2000, he joined TXC Corporation, Taiwan, where he engaged in research and development of a frequency control device. Currently, he is a doctoral candidate at the Institute of Applied Mechanics of National Taiwan University. His current research interests include bulk and surface acoustic wave and advanced quartz crystal frequency control device.

Chi-Yuan Lee received his MS from Tamkang University, Taiwan in 1997, and his PhD degree in Mechanical Engineering from National Taiwan University, Taiwan, in 2004. He is currently an associate professor at the Department of Mechanical Engineering, Yuan Ze University, Taiwan. His research interests are microelectromechanical systems (MEMS), acoustic devices, micro fuel cells, and microreformers.

Yi-Chang Lu received his MS in mechanical engineering from National Taiwan University, Taiwan, in 2007. He is working as a research and development engineer for Asia Pacific Microsystems, Inc., Taiwan. His research interests are MEMS fabrication technology and serving sensors, actuators, inkjet, RF, optical, and biological applications.

Pei-Yen Chen received both his BS and MS in power mechanical engineering from National Tsing Hua University, Hsin-Chu, Taiwan, in 1980 and 1982, and his PhD in theoretical and applied mechanics from Cornell University, Ithaca, New York, in 1990. His PhD dissertation was about the vibration suppression of flexible structures using active feedback control. He has worked in the Chung-Shan Institute of Science and Technology, Tao-Yuan, Taiwan, since 1982. His current research interests are in the areas of MEMS and multidisciplinary coupling study.

Yung-Chung Chin received his MS from Chiao-Tung University, Taiwan, in 1997, and PhD in electronic engineering from Chung Yuan Christian University, Taiwan, in 2008. In 2008, he joined TXC Corporation, as a design engineer at the product research and development center. His research interests in the field currently include MEMS, FBAR, frequency control devices, and oscillator circuits.

Pei-Zen Chang received his BS in civil engineering from National Taiwan University, Taipei, Taiwan, in 1984, and his PhD in theoretical and applied mechanics from Cornell University, Ithaca, New York, in 1991. He then joined the faculty of Institute of Applied Mechanics, National Taiwan University and became a full professor in 1999. His current research interests are in the area of micromachined sensors and actuators.